Mechanism and Kinetics of Direct N_2O Decomposition over Fe−MFI Zeolites with Different Iron Speciation from Temporal Analysis of Products

Evgenii V. Kondratenko*,† and Javier Pérez-Ramírez*,‡

Leibniz-Institut für Katalyse e. V. an der Universität Rostock, Aussenstelle Berlin, Richard-Willstätter-Strasse, 12 D-12489 Berlin, Germany, and Laboratory for Heterogeneous Catalysis, Catalan Institution for Research and Advanced Studies (ICREA) and Institute of Chemical Research of Catalonia (ICIQ), Av. Països Catalans 16, E-43007 Tarragona, Spain

Received: June 6, 2006; In Final Form: August 23, 2006

The mechanism of direct N_2O decomposition over Fe−ZSM-5 and Fe−silicate was studied in the temporal analysis of products (TAP) reactor in the temperature range of 773−848 K at a peak N_2O pressure of ca. 10 Pa. Several kinetic models based on elementary reaction steps were evaluated to describe the transient responses of the reactant and products. Classical models considering oxygen formation via recombination of two adsorbed monoatomic oxygen species (*-O + *-O → O_2 + 2*) or via reaction of N_2O with adsorbed monoatomic oxygen species (N_2O + *-O → O_2 + N_2 + *) failed to describe the experimental data. The best description was obtained considering the reaction scheme proposed by Heyden et al. (*J. Phys. Chem. B* **2005**, *109*, 1857) on the basis of DFT calculations. N_2O decomposes over free iron sites (*) as well as over iron sites with adsorbed monoatomic oxygen species (*-O). The latter reaction originates adsorbed biatomic oxygen species followed by its transformation to another biatomic oxygen species, which ultimately desorbs as gas-phase O_2. In line with previous works, our results confirm that the direct N_2O decomposition is controlled by pathways leading to O_2. Our kinetic model excellently described transient data over Fe−silicalite and Fe−ZSM-5 zeolites possessing markedly different iron species. This finding strongly suggests that the reaction mechanism is not influenced by the iron constitution. The TAP-derived model was extrapolated to a wide range of N_2O partial pressures (0.01−15 kPa) and temperatures (473−873 K) to evaluate its predictive potential of steady-state performance. Our model correctly predicts the relative activities of two Fe−FMI catalysts, but it overestimates the absolute catalytic activity for N_2O decomposition.

1. Introduction

Fe−MFI zeolites are active catalysts for N_2O abatement in tail gases of industrial and energy-related processes.[1−3] For example, Uhde is commercializing the EnviNOx system based on Fe−ZSM-5 for the combined removal of N_2O (by direct decomposition) and NO_x (by NH_3−SCR) in the tail gas of nitric acid plants.[4] The practical relevance of these materials in environmental catalysis as well as in N_2O-mediated selective oxidation of various hydrocarbons stimulated extensive research in the past decade. These studies have aimed at deriving relationships between the preparation method of the zeolite, the nature of the active iron species, and the catalytic performance.[5−16]

The kinetics of direct N_2O decomposition over iron-containing zeolites has also been extensively investigated. Fu et al.[17] described the steady-state rate of N_2O decomposition over Fe−Y by $-dp_{N_2O}/dt = k_{obs}p_{N_2O}$. The results were consistent with an oxygen transfer redox mechanism, in which N_2O simultaneously acts as oxidizing (eq 1) and reducing (eq 2) agent. These authors stated that the rate-determining step is the catalyst reduction by N_2O. The same two-step reaction scheme was also used by Kapteijn et al.[14] to model the steady-state N_2O decomposition over Fe−ZSM-5 in an integral fixed-bed reactor. The rate of N_2O decomposition exhibited a pseudo-first-order behavior with respect to N_2O partial pressure and no inhibition by oxygen. In agreement with ref 17, these authors concluded that O_2 formation, which occurs via the removal of adsorbed oxygen species by N_2O (eq 2), is the slowest step in the overall reaction.

$$N_2O + * \rightarrow N_2 + *\text{-}O \quad (1)$$

$$N_2O + *\text{-}O \rightarrow N_2 + O_2 + * \quad (2)$$

Recent mechanistic studies using transient techniques, which have potential for providing deeper mechanistic insights into complex catalytic reactions, have unequivocally substantiated that O_2 formation is the rate-determining step in N_2O decomposition over iron-containing zeolites.[10,11,18−21] Several reaction pathways leading to O_2 have been put forward. However, they are still debated in the literature and very often qualitatively described. For example, Wood et al.[15] using infrared spectroscopy and temperature-programmed reaction and Ates and Reitzmann[22] using a multipulse transient response method with subsequent temperature-programmed desorption supported the relevance of the reaction of adsorbed *-O species with gas-phase N_2O (eq 2) for O_2 formation over Fe−ZSM-5 zeolites. However, our previous mechanistic studies in the temporal analysis of products (TAP) reactor revealed that N_2 and O_2 were not formed in the same reaction step under transient vacuum conditions.[21,23] On the basis of this, the recombination of two *-O atoms into molecular oxygen (eq 3) was suggested as a

* Corresponding authors. E-mail: evgenii@aca-berlin.de (E.V.K.); jperez@iciq.es (J.P.R.).

† Leibniz-Institut für Katalyse e. V. an der Universität Rostock (former Institute for Applied Chemistry Berlin-Adlershof).

‡ Catalan Institution for Research and Advanced Studies (ICREA) and Institute of Chemical Research of Catalonia (ICIQ).

10.1021/jp063492w CCC: $33.50
Published on Web 10/12/2006

source of O_2 in N_2O decomposition over Fe−MFI. Pirngruber et al.[12] have also supported this conclusion.

$$*\text{-}O + *\text{-}O \rightarrow O_2 + 2* \quad (3)$$

Bulushev et al.[24] have also considered eq 3 as the rate-determining step in their reaction scheme of N_2O decomposition over H−ZSM-5 with low Fe content. Three additional steps were considered: (i) the reversible adsorption of N_2O as the first elementary step (eq 4); (ii) the transformation of adsorbed N_2O into NO (eq 5); (iii) the fast removal of adsorbed oxygen by adsorbed NO leading to O_2 and site regeneration (eq 6). The reversible adsorption of N_2O has been also proposed by Ates and Reitzmann.[22] Equation 5 was supported by TPD[24] as well as by IR studies of Grubert et al.,[25] who observed the formation of nitrosyl groups during interaction of N_2O with Fe−ZSM-5 and Fe−MCM-41.

$$N_2O + * \leftrightarrow *\text{-}N_2O \quad (4)$$

$$*\text{-}N_2O \rightarrow *\text{-}NO + 1/2N_2 \quad (5)$$

$$*\text{-}NO + 2*\text{-}O \rightarrow *\text{-}NO + O_2 + 2* \quad (6)$$

Very recently, Heyden et al.[26,27] have developed a comprehensive mechanistic model for the direct decomposition of N_2O on Fe−ZSM-5 on the basis of DFT calculations. Isolated Fe cations were hypothesized as the active sites in the reaction. Briefly, their mechanism starts with eq 1 yielding $Z^-[FeO]^+$ (*-O) and assumes its successive oxidation by N_2O to $*\text{-}O_2$ (eq 7) and further expanding to $*\text{-}O_3$ (eq 8). These authors concluded that the main reaction pathway for O_2 formation under steady-state conditions is the decomposition of triatomic oxygen species according to eq 9. Their simulations in ref 26 successfully reproduced experimental results of temperature-accelerated desorption of oxygen species deposited over Fe sites upon N_2O decomposition published in the literature. However, these authors did not elaborate on the potential of their kinetic model for describing the steady-state catalytic performance of Fe−ZSM-5.

$$N_2O + *\text{-}O \rightarrow *\text{-}O_2 + N_2 \quad (7)$$

$$N_2O + *\text{-}O_2 \rightarrow *\text{-}O_3 + N_2 \quad (8)$$

$$*\text{-}O_3 \rightarrow *\text{-}O + O_2 \quad (9)$$

Despite the extensive work summarized above, a widely accepted mechanism of direct N_2O decomposition over iron-containing zeolites is not agreed upon. This is an essential aspect to derive rational kinetic models able to predict the catalytic performance and contribute to reactor simulation and design. In this paper, we have combined transient experiments in the temporal analysis of products (TAP) reactor and kinetic modeling of the derived responses of N_2O, N_2, and O_2 for obtaining an improved mechanistic description of the process. Emphasis is an understanding reaction pathways leading to O_2 and N_2 as well as the influence of the iron constitution on the reaction mechanism. To this end, transient experiments were performed at 773−848 K over Fe−ZSM-5 and Fe−silicalite possessing a markedly different iron speciation. Additionally, for the first time, we have evaluated the potential of the TAP-derived kinetic model for prediction of steady-state catalytic performance in direct N_2O decomposition at ambient pressure.

2. Experimental Section

2.1. Catalysts. Isomorphously substituted Fe−ZSM-5 and Fe−silicalite were synthesized hydrothermally followed by calcination and steam treatment, as described elsewhere.[9,16,28] The iron content in steam-treated Fe−ZSM-5 (Si/Al = 31 and 0.67 wt % Fe) and Fe−silicalite (Si/Al ∼ ∞ and 0.68 wt % Fe) was very similar, but the iron speciation in the catalysts differed substantially. Characterization studies[9,16,28] have concluded a rather uniform distribution of iron species in Fe−silicalite, dominated by isolated iron ions in extraframework positions. The degree of iron clustering in steam-activated Fe−ZSM-5 is more prominent; isolated and oligonuclear oxo species in the zeolite pores coexisted with iron oxide nanoparticles of 1−2 nm.

TABLE 1: Kinetic Models Evaluated in This Work

model	elementary reaction step	reaction no.
1	$N_2O + * \rightarrow N_2 + *\text{-}O$	1.1
	$*\text{-}O + *\text{-}O \rightarrow O_2 + 2*$	1.2
2	$N_2O + * \rightarrow N_2 + *\text{-}O$	2.1
	$N_2O + *\text{-}O \rightarrow N_2 + O_2 + *$	2.2
3	$N_2O + * \rightarrow N_2 + *\text{-}O$	3.1
	$*\text{-}O + *\text{-}O \rightarrow *\text{-}O_2 + *$	3.2
	$*\text{-}O_2 \rightarrow O_2 + *$	3.3
4	$N_2O + * \rightarrow N_2 + *\text{-}O$	4.1
	$N_2O + *\text{-}O \rightarrow N_2 + *\text{-}O_2$	4.2
	$*\text{-}O_2 \rightarrow O_2 + *$	4.3
5	$N_2O + * \rightarrow *\text{-}O + N_2$	5.1
	$N_2O + *\text{-}O \rightarrow O\text{-}*\text{-}O + N_2$	5.2
	$O\text{-}*\text{-}O \rightarrow *\text{-}O_2$	5.3
	$*\text{-}O_2 \rightarrow O_2 + *$	5.4
6	$N_2O + * \rightarrow *\text{-}O + N_2$	6.1
	$N_2O + *\text{-}O \rightarrow *\text{-}O_2 + N_2$	6.2
	$N_2O + *\text{-}O_2 \rightarrow *\text{-}O_3 + N_2$	6.3
	$*\text{-}O_2 \rightarrow O_2 + *$	6.4
	$*\text{-}O_3 \rightarrow O_2 + *\text{-}O$	6.5

2.2. Transient Experiments. Mechanistic investigations of N_2O decomposition over the iron-containing zeolites were carried out in the temporal analysis of products (TAP-2) reactor, a transient pulse technique with sub-millisecond time resolution.[29] The sample (50 mg of Fe−silicalite and 30 mg of Fe−ZSM-5, sieve fraction 250−350 μm) was packed in the quartz fixed-bed microreactor (40 mm length and 6 mm i.d.) between two layers of quartz particles of the same sieve fraction. The catalyst was pretreated in flowing He (30 mL STP min^{-1}) at 773 K and atmospheric pressure for 2 h. The pretreated sample was then exposed to vacuum (10^{-5} Pa), and the pulse experiments were subsequently performed. The direct N_2O decomposition was investigated in the temperature range of 773−848 K by pulsing N_2O:Ne = 1:1. Knudsen diffusion describes the transport of the gas in the microreactor at the pulse size applied ($5 \cdot 10^{14}$ molecules). Under this regime, the transient responses are a function of gas−solid interactions; i.e., they are not influenced by eventual collisions of species in the gas phase.

Ne (99.995%) and N_2O (99%) were used without additional purification. A quadrupole mass spectrometer (HAL RC 301, Hiden Analytical) was applied for quantitative analysis of reactants and reaction products. The transient responses at the reactor outlet were monitored at the following atomic mass units (amu): 44 (N_2O), 32 (O_2), 30 (N_2O), 28 (N_2, N_2O), and 20 (Ne). In the experiments, 10 pulses for each amu were recorded and averaged to improve the signal-to-noise ratio. The variations in feed components and reaction products were determined from the respective amus using standard fragmentation patterns and sensitivity factors.

3. Kinetic Evaluation of Transient Experiments

3.1. Kinetic Models for N_2O Decomposition. The kinetic models of direct N_2O decomposition evaluated in this work are summarized in Table 1. The reaction steps postulated in these

models were taken from previous experimental and theoretical studies.[13,17,20,24,27,37] Since Fe−MFI zeolites pretreated in flowing He at 773 K and exposed to vacuum (see section 2.2) possess iron species without any adsorbed oxygen species, N_2O decomposition is initiated over free iron sites (*) in all the models. On the basis of previous kinetic studies,[13,17,20,24,27,37] models 2, 4, and 5 additionally consider that iron sites with deposited monoatomic oxygen species (*-O) are active for N_2O decomposition too. Moreover, model 6 also includes N_2O decomposition over iron sites with adsorbed biatomic oxygen species (*-O_2), as proposed in ref 27 using DFT calculations. As an example, the below equations represent the mass balance for the gas-phase and surface species for model 2:

$$\frac{\partial C_{N_2O}}{\partial t} = D_{eff}\frac{\partial^2 C_{N_2O}}{\partial x^2} - C_{total}k_1 C_{N_2O}(1-\Theta_{*-O}) - C_{total}k_2 C_{N_2O}\Theta_{*-O}$$

$$\frac{\partial C_{N_2}}{\partial t} = D_{eff}\frac{\partial^2 C_{N_2}}{\partial x^2} + C_{total}k_1 C_{N_2O}(1-\Theta_{*-O}) + C_{total}k_2 C_{N_2O}\Theta_{*-O}$$

$$\frac{\partial C_{O_2}}{\partial t} = D_{eff}\frac{\partial^2 C_{O_2}}{\partial x^2} + C_{total}k_2 C_{N_2O}\Theta_{*-O}$$

$$\frac{\partial \Theta_{*-O}}{\partial t} = k_1 C_{N_2O}(1-\Theta_{*-O}) - k_2 C_{N_2O}\Theta_{*-O}$$

Here D_{eff} is the effective Knudsen diffusion coefficient, k_i is the rate coefficient, C_{total} is the total number of active sites, and Θ_i is the coverage of surface species. The balance of surface species can be expressed by

$$\Sigma\Theta_i = \Theta_{*-O} + \Theta_* = 1$$

where Θ_* is the fraction of free active sites and Θ_{*-O} is the fraction of adsorbed monoatomic oxygen species. Similar expressions can be derived for other models in Table 1.

The intracrystalline diffusion was not taken into consideration in all the models. This simplification is based on the following facts. Keipert and Baerns[30] have previously shown that this process has a very slight influence on the shape of transient responses of inert gases upon pulsing in the TAP reactor. The transport behavior of oxygen and nitrogen may be considered to be similar to inert gases. Therefore, the transport of gases inside the microreactor was described by Knudsen diffusion along the reactor axis. The apparent values of Knudsen diffusion coefficient were estimated over the relevant range of temperatures from fitting of neon transient responses assuming Knudsen diffusion model (first term in the above equations for gas-phase species). The obtained coefficients were fixed and used to further calculate the respective values for N_2O, N_2, and O_2 according to eq 10

$$D_i^{eff} = D_{Ne}^{eff}\sqrt{M_{Ne}/M_i} \quad (10)$$

where D_{Ne}^{eff} is the effective Knudsen diffusion coefficient of Ne. M_{Ne} and M_i are the molecular weights of Ne and the other gas-phase components, respectively.

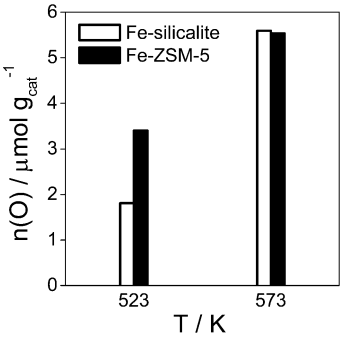

Figure 1. Amount of oxygen irreversibly adsorbed on the iron-containing zeolites upon N_2O multipulsing in the TAP reactor.

3.2. Parameter Estimation. The parameter estimation procedure used here was described elsewhere.[31,32] Briefly, it is based on a numerical solution of partial differential equations (PDEs) describing processes of diffusional transport, adsorption/desorption, and reaction in the TAP microreactor. PDEs are transformed into coupled ordinary differential equations (ODEs) by a spatial approximation and then integrated numerically using the PDEONE routine.[33] Parameters were determined using first a genetic algorithm to find good starting values[34] and then the Nelder−Mead simplex algorithm.[35] The TAP microreactor was described as a one-dimensional pseudohomogeneous system divided into three different zones, which are represented by the catalyst and the two layers of inert material where the zeolite was sandwiched. The catalyst is located in the isothermal zone of the reactor. The goodness of fit was determined by an objective function defined as the sum of squares of the shortest deviations between the respective pairs of points of the experimental and simulated transient responses.[32] For simultaneous fitting of transient responses of various intensities, the number of the representative points for low-intensity responses was higher than for more intensive ones. This procedure is appropriate to minimize the influence of highly intensive responses on the objective function.

4. Results and Discussion

4.1. N_2O Decomposition under Transient Conditions. Steam-activated Fe−silicalite and Fe−ZSM-5, which are active catalysts for direct N_2O decomposition at ambient pressure,[16,21] decompose N_2O under vacuum conditions, too. Gas-phase N_2 was observed above 523 K. However, gas-phase O_2 was only detected above 623 K. This means that oxygen species originated upon N_2O decomposition stay on the catalyst surface below 623 K. On the basis of this experimental observation, the concentration of active sites for N_2O activation ($N_2O + * \rightarrow N_2 + *\text{-}O$) was estimated by multipulse experiments at 523 and 573 K, according to the procedure described elsewhere.[36] The obtained results are presented in Figure 1. From this figure it is clear that the concentration of active sites for N_2O activation is comparable for both samples. Despite this fact, the direct N_2O decomposition behavior of the catalysts above 723 K differs substantially, where both N_2 and O_2 were observed as reaction products.

The transient responses of O_2 and N_2 obtained upon N_2O pulsing over Fe−silicalite and Fe−ZSM-5 are shown in Figure 2. They were height-normalized for a better comparison of the shapes (broadness of transient response) and the order of appearance of products. The latter is characterized by the time of maximum of the transient response (t_{max}). This parameter

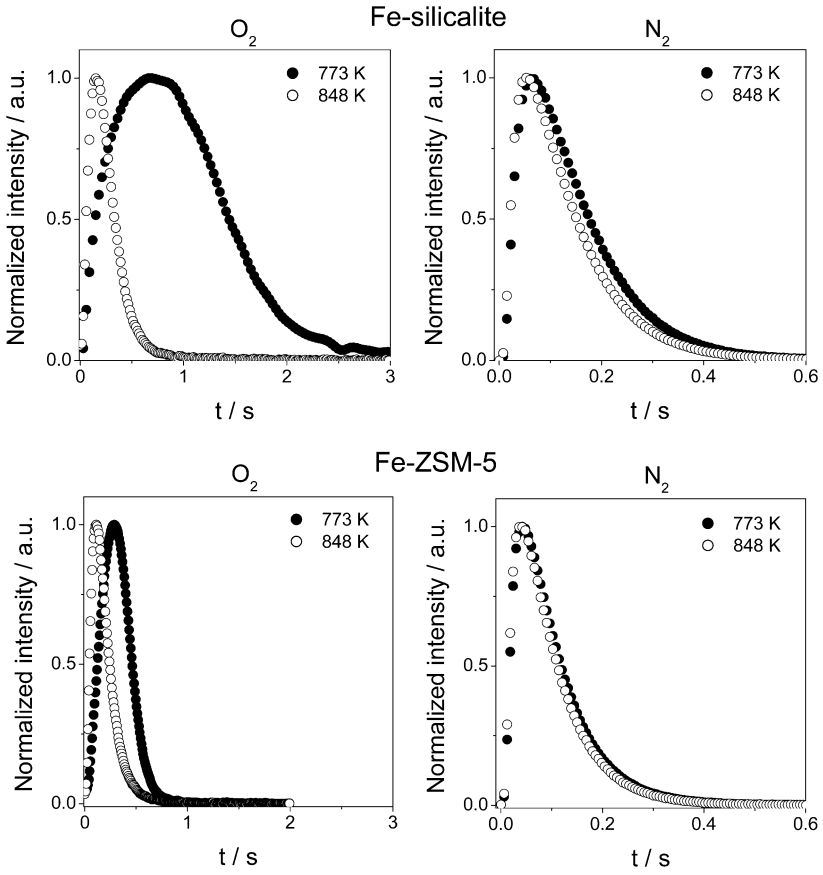

Figure 2. Normalized O_2 and N_2 transient responses upon direct N_2O decomposition over the iron-containing zeolites.

contains relevant mechanistic and kinetic information on chemical and transport phenomena inside the reactor.[29]

The N_2 transient responses in Figure 2 appear at considerably shorter time (t_{max} = 0.037−0.06 s) than those of O_2 (t_{max} = 0.11−0.67 s). Moreover, the t_{max} of O_2 was shorter over Fe−ZSM-5 (t_{max} = 0.28 s at 773 K) as compared to Fe−silicalite (t_{max} = 0.68 s at 773 K). However, the t_{max} values of N_2 are similar over both catalysts. The temperature hardly impacts the t_{max} of N_2, contrarily to the strong dependence of the t_{max} of O_2 on this variable. Upon increase of the reaction temperature from 773 to 848 K, the t_{max} of O_2 over Fe−silicalite and Fe−ZSM-5 decreased from 0.28 to 0.11 s and from 0.67 to 0.14 s, respectively. These results provide valuable qualitative information on the reaction mechanism: (i) Reaction pathways leading to oxygen formation are slower than those of nitrogen, and (ii) oxygen formation is generally much easier over Fe−ZSM-5 than over Fe−silicalite. The sub-millisecond time resolution of the TAP technique made it possible to derive such conclusions. To quantify the above statements, a detailed kinetic analysis of the reaction is elaborated in the next section.

4.2. Kinetics of N_2O Decomposition. The kinetics of direct N_2O decomposition was analyzed to derive insights into plausible reaction pathways leading to N_2 and O_2. As elaborated in the Introduction, this aspect has been extensively debated in the literature.[12,14,17,21,23] To this end, the transient responses of N_2O, N_2, and O_2 derived from pulse experiments in the TAP reactor were simultaneously fitted to different kinetic models in Table 1. These models basically differ in reaction pathways leading to O_2. Models 1 and 2 consider classical O_2 formation via recombination of two monoatomic *-O species[10,14] and via a direct reaction of gas-phase N_2O with *-O,[17] respectively. These two pathways are modified in models 3 and 4 assuming oxygen formation via decomposition of a bimolecular oxygen precursor, which was previously suggested.[20,38,39] On the basis of recent DFT modeling of N_2O decomposition over Fe−ZSM-5,[27] biatomic oxygen species of different structure (denoted O-*-O and *-O_2) and triatomic oxygen species (*-O_3) were additionally taken as surface precursors of gas-phase O_2 in models 5 and 6, respectively. It has to be stressed that our modeling approach provides no insights into the structure and/or oxidation state of the active iron sites in the zeolite or the charge of adsorbed oxygen species.

Fe−Silicalite. Figure 3 displays the experimental transient responses of N_2O, N_2, and O_2 upon pulsing N_2O over Fe−silicalite at 798 K and the resulting calculated responses by applying models 1−6 with optimized kinetic parameters. Models 1 and 3, where recombination of two adsorbed monoatomic oxygen species plays a dominant role in O_2 formation, failed to describe the experimental data. Models 2 and 4 considering O_2 formation via reaction of N_2O with adsorbed oxygen species describe the O_2 transient response better than models 1 and 3. However, the experimental N_2O and N_2 responses were poorly predicted. Accordingly, classical kinetic schemes for N_2O decomposition unsuccessfully describe the TAP experiments.

DFT-derived pathways of O_2 formation were considered in models 5 and 6. These studies postulated the existence of adsorbed mono-, bi-, and triatomic oxygen species on the catalyst surface. The existence of different adsorbed oxygen species upon N_2O decomposition over Fe−silicalite is experimentally supported. Without statement on the nature of oxygen species, we have recently suggested two adsorbed oxygen species, to explain the dependence of the degree of propane[21] and methane[40] conversion over Fe−silicalite on the time delay between nitrous oxide and hydrocarbon pulses in the TAP reactor. This concept is in agreement with the results of Kunimori et al.,[41−43] who postulated two types of oxygen species originated upon N_2O

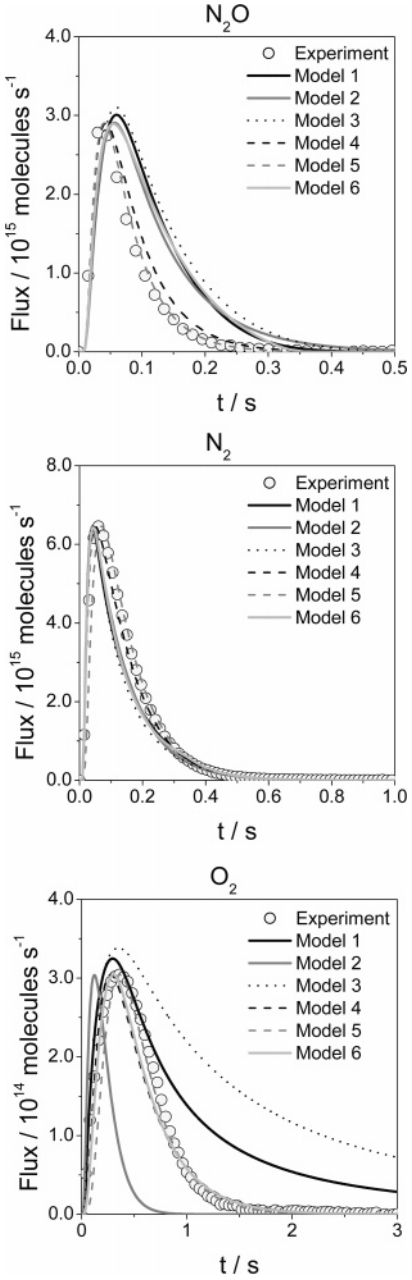

Figure 3. Experimental (symbols) and calculated (lines) transient responses of N_2O, N_2, and O_2 upon N_2O decomposition over Fe−silicalite at 798 K.

activation over Fe−beta during SCR with CH_4. Using models 5 and 6, an improved description of the O_2 transient response was attained. As shown in Figure 3, the smallest deviations between the experimental and predicted transient responses of N_2O, N_2, and O_2 were obtained with model 5. This model considers N_2O decomposition over free iron sites yielding gas-phase N_2 and iron site with monoatomic adsorbed oxygen species (Table 1, step 5.1). The latter one is able to decompose a second N_2O molecule with formation of a biatomic oxygen species (Table 1, step 5.2). Heyden et al.[27] proposed an O−Fe−O structure for this intermediate, which can be transformed to another biatomic oxygen species, where oxygen atoms are chemically bound (Table 1, step 5.3). The final step of the catalytic cycle is the decomposition of the latter biatomic oxygen species, yielding gas-phase O_2 (Table 1, step 5.4) and a free iron site (*).

Several authors have suggested the reversible N_2O adsorption (eq 4) as the first step in the mechanism of nitrous oxide decomposition over iron-containing ZSM-5 zeolites.[22,24] However, extension of model 5 with two additional reaction pathways (adsorption and desorption of N_2O) did not improve the description of our experimental results. Accordingly, we suggest the relatively minor importance of these steps under TAP conditions.

On the basis of the results of the model discrimination at the reference temperature, model 5 was selected to describe the transient responses at other temperatures in the range of 773−848 K. To reduce the correlation between activation energies and preexponential factors,[44,45] activation energies for all elementary reaction steps were derived according to eq 11:

$$k_{T_i} = k_{T_{ref}} \exp\left(-\frac{E_a}{R}\left(\frac{1}{T_i} - \frac{1}{T_{ref}}\right)\right) \qquad (11)$$

Here T_{ref} and $k_{T_{ref}}$ are the reference temperature and rate coefficient at this temperature, respectively. According to ref 44, the reference temperature should be intermediate within the temperature range applied. In the present study, 798 K was chosen as the reference temperature.

The rate coefficients at the reference temperature were initially obtained from fitting as described above and fixed. The model-predicted and experimental responses of N_2O, N_2, and O_2 obtained over Fe−silicate at various temperatures are compared in Figure 4. Model 5 excellently described the profiles of reactant and products. Exceptionally, small deviations between experimental and calculated values were noticed in the O_2 profile at 773 K.

Fe−ZSM-5. As encountered in Fe−silicalite, models 1 and 3 did not properly describe the transient responses of N_2O, N_2 and O_2 over Fe−ZSM-5. An improved fitting was obtained using models 2, 4, and 6, particularly for the O_2 transient response. The reaction scheme in model 5 again provided the best description of all transient responses in the temperature range investigated (Figure 4).

In summary, for both catalysts studied, the recombination of two monoatomic oxygen species (*-O) yielding directly gas-phase O_2 (model 1) or resulting in the formation of a surface biatomic adsorbed precursor of gas-phase O_2 (model 3) can be excluded as the reaction pathways of O_2 formation in N_2O decomposition. Besides, the classical scavenging mechanism of N_2O decomposition in eqs 1 and 2 is also not appropriate either. In agreement with previous works,[14,17,26,27] our kinetic evaluation predicts that iron sites with deposited monoatomic oxygen species are also active for N_2O decomposition. Oxygen formation occurs via two steps: (i) A biatomic oxygen precursor is formed upon N_2O decomposition over iron site with monoatomic adsorbed oxygen species. (ii) This biatomic precursor is transformed to another biatomic oxygen species, which decomposes yielding gas-phase O_2 and free iron site. The importance of triatomic oxygen species in oxygen formation as proposed by Heyden et al.[26,27] is not substantiated by our modeling. It has to be stressed that the different iron speciation in Fe−silicalite and Fe−ZSM-5 does not influence the mechanistic scheme of N_2O decomposition.

4.3. Influence of the Iron Speciation on the Kinetic Parameters. The optimized kinetic parameters of direct N_2O decomposition resulting from model 5 over Fe−silicalite and Fe−ZSM-5 are compared in Table 2. It has to be mentioned that it is not possible to determine independently the rate coefficient (k_i) of reaction pathways 1 and 2 in model 5 and the total number of active catalyst sites (C_{total}). Therefore, apparent rate coefficients ($k_i C_{total}$) were obtained. For both zeolites, the

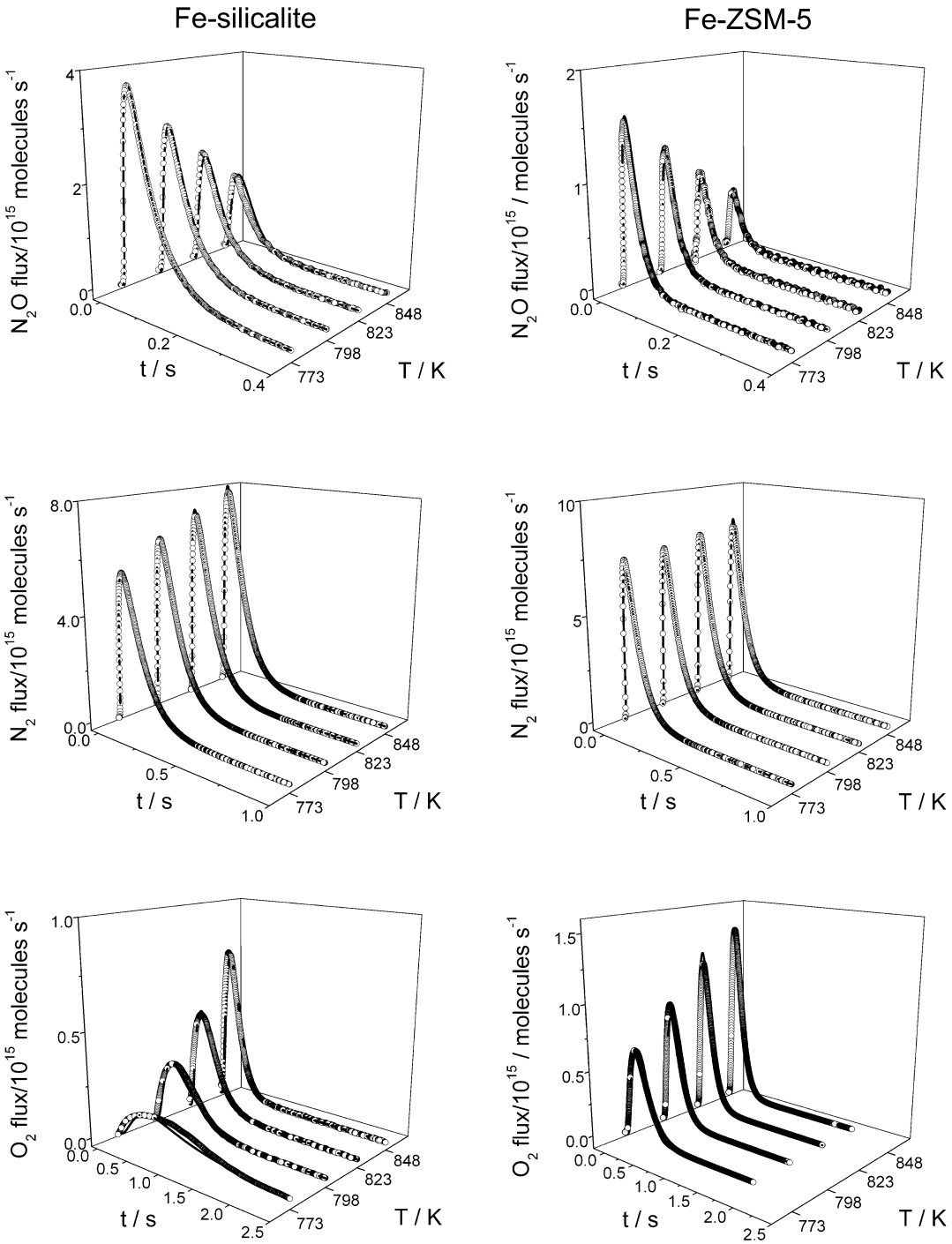

Figure 4. Experimental (symbols) and calculated (lines) transient responses of N_2O, N_2, and O_2 using model 5 upon N_2O decomposition over Fe−silicalite and Fe−ZSM-5 at different temperatures.

TABLE 2: Kinetic Parameters for the Elementary Reaction Steps of Direct N_2O Decomposition over Fe−Silicalite and Fe−ZSM-5 Using Model 5 (Table 1)

		k_{798K}/s^{-1}		E_a/kJ mol^{-1}		
no.	elementary reaction steps	Fe−Silicalite	Fe−ZSM-5	Fe−Silicalite	Fe−ZSM-5	ref 27
1	$N_2O + * \rightarrow *\text{-}O + N_2$[a]	1200	3700	120	69	0
2	$N_2O + *\text{-}O \rightarrow O\text{-}*\text{-}O + N_2$[a]	170	1700	81	98	115−130
3	$O\text{-}*\text{-}O \rightarrow *\text{-}O_2$	26	20	298	142	60−93
4	$*\text{-}O_2 \rightarrow O_2 + *$	2.7	11	125	50	215

[a] For these reaction steps, the rate coefficient is the product of the intrinsic rate coefficient and the total number of active sites.

reaction pathways leading to gas-phase O_2 have the lowest rate constant, which is up to 400 times lower than the rate constant of N_2 formation. Moreover, the activation energies of these reaction pathways are higher than those leading to N_2. This is in good correspondence with the experimental observations in Figure 2; the time of maximum of oxygen transient response is more strongly influenced by temperature as compared to that of nitrogen.

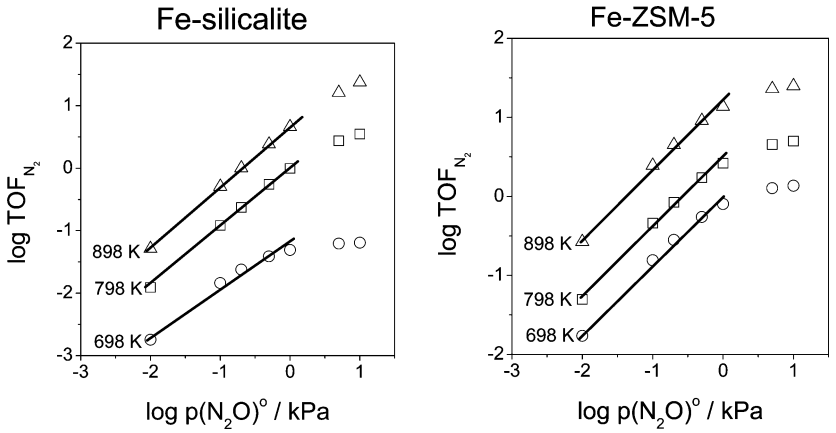

Figure 5. Predicted turnover frequencies of N_2 formation upon N_2O decomposition over Fe−silicalite and Fe−ZSM-5 at N_2O partial pressures and temperatures in the range of $1-10^4$ Pa and 698−898 K, respectively. Calculations were performed using the kinetic parameters in Table 2.

Taking into account the activation energies of reaction pathways 3 and 4 in Table 2, it is concluded that oxygen formation occurs easier over Fe−ZSM-5 (50−142 kJ mol^{-1}) than over Fe−silicalite (125−300 kJ mol^{-1}). This is in agreement with our experimental observations in Figure 2. On the basis of the experimental data and the results of kinetic fitting, oxygen formation can be considered as the rate-limiting step in N_2O decomposition under the experimental conditions in this study. Analysis of kinetic parameters indicates that not only O_2 formation but also N_2 formation (steps 1 and 2 in Table 2) is influenced by the catalyst. According to the TAP-derived model, Fe−silicalite is up to 10 times less active than Fe−ZSM-5. This is in good agreement with previously reported results of N_2O decomposition in a broad range of temperatures and N_2O partial pressures.[16,21]

The fitted activation energies of all the elementary reaction steps have been compared with those determined from DFT modeling,[27] since no experimental data are available. The most significant difference was found for N_2O decomposition over free iron sites. The DFT calculations predict zero activation energy, while activation energies of 120 and 70 kJ mol^{-1} were obtained from our kinetic evaluation for Fe−silicalite and Fe−ZSM-5, respectively. There is reasonable agreement between DFT calculations (115−130 kJ mol^{-1}) and results from our TAP-derived model (80−100 kJ mol^{-1}) with respect to the activation energies of N_2O decomposition over iron sites with adsorbed mono-atomic oxygen species (*-O). The activation energy for transformation of O-*-O species into *-O_2 (step 3 in Table 2) over Fe−ZSM-5 (142 kJ mol^{-1}) is close to that predicted by DFT for Fe−ZSM-5 (93 kJ mol^{-1}). However, the corresponding activation energy over Fe−silicalite is considerably higher (300 kJ mol^{-1}). The difference between Fe−ZSM-5 and Fe−silicalite can be tentatively attributed to the different constitution of the catalysts with respect to iron. Generally, both approaches (DTF and transient kinetics fitting) conclude that activation energies of reaction pathways of N_2O decomposition are lower than that of O_2 formation. However, in contrast to the previous DFT calculations, our kinetic analysis predicts in agreement with the experiment that the decomposition of biatomic oxygen species results in O_2 formation under transient vacuum conditions. This process is easier over Fe−ZSM-5 than over Fe−silicalite. This is tentatively attributed to the structure of the iron sites as well as due to the redox behavior of the active catalytic centers. As reported elsewhere,[9,16,28] Fe−ZSM-5 contains a large fraction of iron as oligonuclear species coexisting with isolated iron sites and iron oxide nanoparticles (1−2 nm), while Fe−silicalite mainly consists of isolated iron sites. The iron species in the former sample display a higher redox activity than in Fe−silicalite due to the lower concentration of Fe^{2+} sites in the latter sample as concluded from in-situ UV/vis.[46] On the basis of our results, it can be stated that there is no fundamental difference between the different iron sites and zeolite matrixes concerning the mechanism of N_2O decomposition. Only the contribution of fast and slow O_2 desorption process seems to distinguish the iron species. This agrees with ref 28; all iron sites, excluding large Fe_2O_3 clusters, contribute to the catalyst activity to a smaller or larger extent.

4.4. Rate-Determining Step and Active Sites under Steady-State Ambient Pressure Conditions. As discussed above, the derived mechanism of N_2O decomposition correctly predicts the transient behavior of N_2O decomposition over samples containing different iron species. The next criterion, which the model should fulfill, is the dependence of the rate of N_2O decomposition on N_2O partial pressure. To this end, the TOF (turnover frequency) for N_2 formation under steady-state conditions was computed taking the parameters in Table 2. The calculations were performed in the temperature range of 698−898 K and N_2O partial pressure range of $(1-15) \times 10^3$ Pa. The calculated TOFs, which are presented in Figure 5, show that the rate of N_2O decomposition is first order in N_2O partial pressure in the range of $1-10^3$ Pa. Above 10^3 Pa, the apparent order of N_2O decomposition decreases. This result is in disagreement with early studies by Hall and co-workers over Fe−Y zeolite[17] and over Fe−mordenite.[47] Unfortunately, no kinetic data on N_2O decomposition over steam-activated Fe−silicalite or Fe−ZSM-5 catalysts at high N_2O partial pressures are available. Accordingly, the correctness of our model prediction cannot be definitively confirmed. However, indirect support for our model can be obtained from the kinetic analysis by Kapteijn et al.[14] over ion-exchanged Fe−ZSM-5. These authors reported that even at relatively low N_2O partial pressures (60−150 Pa), the reaction order over ion-exchanged Fe−ZSM-5 with respect to N_2O was <1 above 733 K.

To further analyze the effect of the N_2O partial pressure on the overall reaction of N_2O decomposition, surface coverages were calculated at different N_2O partial pressures and temperatures. The coverage by free iron sites and iron sites with monoatomic oxygen species practically did not depend on N_2O partial pressure in the range from 1 to 10^3 Pa but decreases upon further pressure increase. In contrast, the coverage by biatomic oxygen species continuously increases with the N_2O partial pressure. Figure 6 shows the TOF (N_2) and coverage by *-O_2 calculated for Fe−silicalite and Fe−ZSM-5 at 798 K and different inlet N_2O partial pressures. Both magnitudes increase

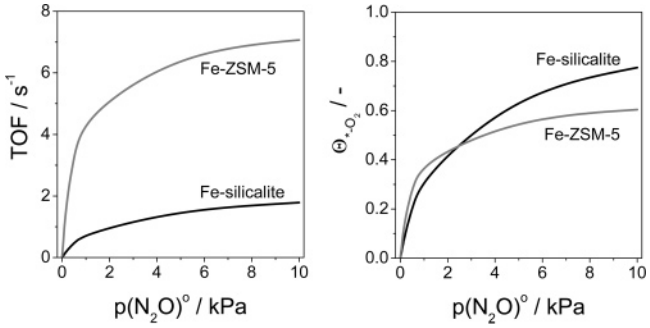

Figure 6. Calculated turnover frequencies of N_2 formation and coverages by *-O_2 upon direct N_2O decomposition over Fe−silicalite and Fe−ZSM-5 at 798 K and different inlet partial pressures of N_2O.

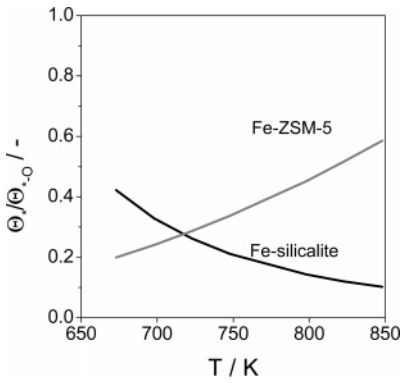

Figure 7. Predicted ratios between the coverage of free iron sites (Θ_*) and iron sites with deposited oxygen monoatomic species (Θ_{*-O}) over the Fe−MFI catalysts at different temperatures. Model 5 was used for calculations.

linearly with the N_2O partial pressure up to 10^3 Pa but only slightly grow when that partial pressure is exceeded.

Three important results from our modeling should be especially emphasized: (i) the lower value of kinetic parameters (up to 400 times) for reaction pathways leading to O_2 as compared to N_2; (ii) little influence of N_2O partial pressure (from 1 to 10^3 Pa) on the fraction of active sites (* and *-O) for N_2O decomposition; and (iii) similar dependence of TOF for N_2 formation and the coverage by *-O_2 (precursor species of gas-phase O_2) species on the N_2O partial pressure. On the basis of the above discussion, it is concluded that the global N_2O decomposition reaction is limited by reaction pathways leading to gas-phase oxygen in agreement with many experimental studies.[10,11,18−21] Differently, Heyden et al.[26] claimed that O_2 desorption cannot be rate limiting, since the catalyst surface would be saturated with oxygen species and N_2O decomposition would be zero order with respect to N_2O partial pressure. Our modeling predicts that this conclusion could be valid at high N_2O partial pressures.

To derive insights into active sites (free Fe species or Fe species with deposited monoatomic oxygen species) actively participating in direct N_2O decomposition under steady-state conditions, the relative ratio of these surface sites was calculated at different temperatures (Figure 7). In contrast to Fe−silicalite, the ratio of Θ_*/Θ_{*-O} for Fe−ZSM-5 increased with temperature. The difference is due to different temperature dependence of the reaction pathways 1 and 2 in Table 2. However, for both catalysts, this ratio is in the range of ca. 0.1−0.5, indicating that none of the active species for N_2O decomposition dominates significantly over the other. On the basis of this fact, it is put forward that the contribution of both free iron sites and iron sites with deposited oxygen species in N_2O decomposition under steady-state conditions is similar.

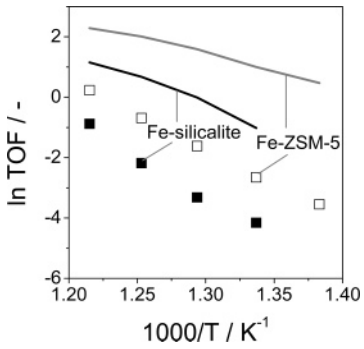

Figure 8. Arrhenius plot of the experimental (symbols) and calculated (lines) turnover frequencies of N_2 formation upon N_2O decomposition over Fe−silicalite and Fe−ZSM-5 at an inlet partial pressure of N_2O of 15000 Pa in the temperature range 748−823 K.

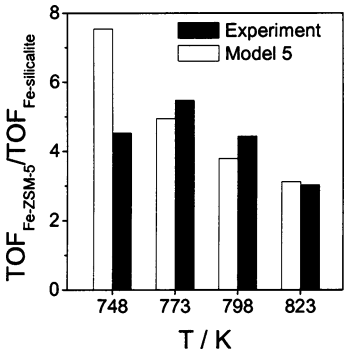

Figure 9. Ratios between the turnover frequencies of N_2 formation over Fe−ZSM-5 and Fe−silicalite in direct N_2O decomposition at different temperatures determined from data in Figure 8.

4.5. Evaluation of the TAP-Derived Model for Predicting Steady-State Performances. The final part of this manuscript aims at examining the applicability of our transient kinetic model to predict the previously reported steady-state performance of Fe−silicalite and Fe−ZSM-5 in direct N_2O decomposition.[21] To this end, we calculated the TOF of N_2 formation under steady-state conditions using an N_2O partial pressure of 15×10^3 Pa in the temperature range 723−823 K. All iron in the catalysts was assumed to be active for direct N_2O decomposition. Such an assumption underestimates the real TOF since not all iron species are active. It should be recalled that the TAP-derived kinetic model is based on the experimental data at peak pressures N_2O of ca. 10 Pa, i.e., 1500 times lower than that often present in e.g. tail gases of nitric acid plants. The simulated TOF values and those calculated from the previously reported steady-state rates of nitrogen formation[21] are compared in Figure 8. As expected, our model overestimates the experimentally determined TOF values. For example, the predicted TOF value at 798 K (reference temperature in our calculations) is 20 times higher than the experimental value. The low experimental TOF values may be due to the fact that, for their calculations, all iron species in the catalysts were assumed to be active for N_2O decomposition. Moreover, the differences between the predicted and experimental TOF values can be related to the experimental conditions. In the present transient study of N_2O decomposition, the catalysts were pretreated in a He flow at 773 K followed by catalyst evacuation to 10^{-5} Pa, while no catalyst pretreatment was performed in our previous steady-state ambient pressure tests.[21] Pirngruber and Roy[37] have reported that high-temperature (above 673 K) pretreatment of Fe−ZSM-5 in He increased its activity toward N_2O decomposition. An indirect support for the above discussion is illustrated in Figure 9. This figure compares the relative ratios of experimentally determined and simulated

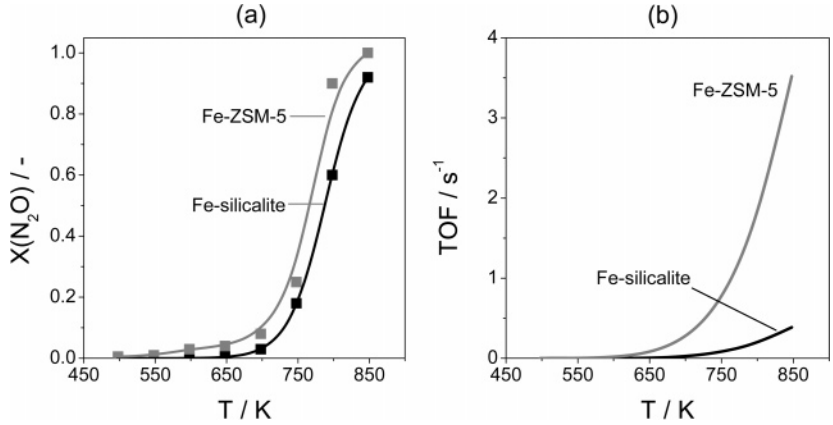

Figure 10. Experimental N_2O conversion (a) and calculated turnover frequencies of N_2 formation (b) over Fe−silicalite and Fe−ZSM-5 at N_2O partial pressure of 150 Pa and different temperatures. Model 5 was used for calculations. Experimental values were taken from ref 16.

TOF's over Fe−ZSM-5 and Fe−silicalite at different temperature. It is clear that the model can reasonably predict the differences in the catalytic activity of isolated iron species and oligonuclear iron sites for N_2O decomposition.

Our kinetic model was not able to accurately reproduce the temperature dependence of the TOF values. The measured apparent activation energies of nitrogen formation over Fe−silicalite and Fe−ZSM-5 were 226 and 190 kJ mol^{-1}, respectively, while the corresponding predicted values are 145 and 92 kJ mol^{-1}. It is clear that the kinetic model underestimates the apparent activation energies. However, it predicts lower apparent activation of N_2O formation over Fe−ZSM-5 as compared to Fe−silicalite in agreement with ref 21. The difference between the predicted and measured temperature dependency of N_2 formation in Figure 8 could be related to the effect of water vapor on N_2O decomposition. Heyden et al.[27] claimed that the apparent activation energy of N_2O decomposition over isolated iron sites in Fe−ZSM-5 increases from ca. 110 kJ mol^{-1} in the absence of water to 230 kJ mol^{-1} in the presence of 100 ppb water. Our transient experiments were performed with very low N_2O pulses (5×10^{14} molecules) in a vacuum, where the influence of water on N_2O decomposition can be neglected. In fact, our kinetic model does not include any influence of water on N_2O decomposition. However, the presence of traces of steam during steady-state ambient pressure tests in ref 21 cannot be excluded.

In the following we compare the measured activity of Fe−silicalite and Fe−ZSM-5[16] in direct N_2O decomposition in a broad temperature range with the calculated ones. The results in Figure 10a exemplify the N_2O conversion over the zeolites at different temperatures and partial pressure of N_2O of 150 Pa. It is clear that independently of the N_2O partial pressure (15 000 Pa (Figure 8) or 150 Pa), Fe−ZSM-5 is more active than Fe−silicalite. The calculated TOF values of N_2 formation are displayed in Figure 10b. In agreement with the experiment, the model predicts higher activity of Fe−ZSM-5 in the whole temperature range as compared to Fe−silicalite.

The above discussions clearly demonstrated the predictive potential of transient kinetic analysis in the TAP reactor. The kinetics of N_2O decomposition derived from low-pressure studies can be extrapolated to higher pressures within the limits of the low coverage conditions. It correctly predicts the differences in steady-state performance of Fe−silicalite and Fe−ZSM-5 catalysts possessing different iron species in the direct N_2O decomposition over a wide range of temperatures and N_2O partial pressures.

5. Conclusions

Transient studies of N_2O decomposition over Fe−silicalite and Fe−ZSM-5 possessing markedly different iron constitution were performed in the TAP reactor at temperatures of 773−848 K using a peak N_2O pressure of 10 Pa. The obtained transient responses of N_2O, N_2, and O_2 were simultaneously fitted to different kinetic models including surface steps with the aim to derive insights into the mechanism of N_2 and O_2 formation. On the basis of model discrimination, it is concluded that there is no fundamental difference in the mechanism of N_2O decomposition between the isolated and oligomeric iron−oxo species. According to the developed kinetic model, there are two reaction pathways of N_2 formation: (i) N_2O decomposes over free iron sites yielding gas-phase N_2 and the iron site with adsorbed monoatomic oxygen. (ii) This oxidized site is also catalytically active for N_2O decomposition leading to gas-phase N_2 and adsorbed biatomic oxygen species. The latter oxygen intermediate isomerizes and further decomposes to give gas-phase O_2 and the free iron site. Reaction pathways leading to oxygen formation are rate limiting. The TAP-derived kinetic model can be used to predict the relative steady-state catalytic performance in direct N_2O decomposition in a wide range of temperatures and N_2O partial pressures.

Acknowledgment. E.V.K. thanks the financial support from the Deutsche Forschungsgemeinschaft (DFG) in the frame of the competence network (Sonderforschungsbereich 546) "Structure, dynamics and reactivity of transition metal oxide aggregates". J.P.R. thanks the Spanish DGICYT for financial support (Project CTQ2006-01562/PPQ).

References and Notes

(1) Pérez-Ramírez, J.; Kapteijn, F.; Mul, G.; Moulijn, J. A. *Chem. Commun.* **2001**, 693−694.

(2) Pérez-Ramírez, J.; Kapteijn, F.; Mul, G.; Xu, X.; Moulijn, J. A. *Catal. Today* **2002**, *76*, 55.

(3) Pérez-Ramírez, J.; Kapteijn, F.; Schöffel, K.; Moulijn, J. A. *Appl. Catal., B* **2003**, *44*, 117.

(4) Groves, M. C. E.; Mauer, R. *Proc. Int. Fert. Soc.* **2004**, *539*, 1.

(5) Kogel, M.; Monnig, R.; Schwieger, W.; Tissler, A.; Turek, T. *J. Catal.* **1999**, *182*, 470.

(6) Centi, G.; Vazzana, F. *Catal. Today* **1999**, *53*, 683.

(7) Marturano, P.; Drozdova, L.; Kogelbauer, A.; Prins, R. *J. Catal.* **2000**, *192*, 236.

(8) Dubkov, K. A.; Ovanesyan, N. S.; Shteinman, A. A.; Starokon, E. V.; Panov, G. I. *J. Catal.* **2002**, *207*, 341.

(9) Pérez-Ramírez, J.; Mul, G.; Kapteijn, F.; Moulijn, J. A.; Overweg, A. R.; Doménech, A.; Ribera, A.; Arends, I. W. C. E. *J. Catal.* **2002**, *207*, 113.

(10) Pérez-Ramírez, J.; Mul, G.; Kapteijn, F.; Moulijn, J. A. *J. Catal.* **2002**, *208*, 211.
(11) Kiwi-Minsker, L.; Bulushev, D. A.; Renken, A. *J. Catal.* **2003**, *219*, 273.
(12) Pirngruber, G. D.; Luechinger, M.; Roy, P. K.; Cecchetto, A.; Smirniotis, P. *J. Catal.* **2004**, *224*, 429.
(13) Kiwi-Minsker, L.; Bulushev, D. A.; Renken, A. *Catal. Today* **2005**, *110*, 191.
(14) Kapteijn, F.; Marban, G.; Rodriguez-Mirasol, J.; Moulijn, J. A. *J. Catal.* **1997**, *167*, 256.
(15) Wood, B. R.; Reimer, J. A.; Bell, A. T. *J. Catal.* **2002**, *209*, 151.
(16) Pérez-Ramírez, J.; Kapteijn, F.; Groen, J. C.; Doménech, A.; Mul, G.; Moulijn, J. A. *J. Catal.* **2003**, *214*, 33.
(17) Fu, C. M.; Korchak, V. N.; Hall, W. K. *J. Catal.* **1981**, *68*, 166.
(18) Mul, G.; Pérez-Ramírez, J.; Kapteijn, F.; Moulijn, J. A. *Catal. Lett.* **2001**, *77*, 7.
(19) Pirngruber, G. D. *J. Catal.* **2003**, *219*, 456.
(20) Wood, B. R.; Reimer, J. A.; Bell, A. T.; Janicke, M. T.; Ott, K. C. *J. Catal.* **2004**, *224*, 148.
(21) Kondratenko, E. V.; Pérez-Ramírez, J. *Appl. Catal., A* **2004**, *267*, 181.
(22) Ates, A.; Reitzmann, A. *J. Catal.* **2005**, *235*, 164.
(23) Pérez-Ramírez, J. *J. Catal.* **2004**, *227*, 512.
(24) Bulushev, D. A.; Kiwi-Minsker, L.; Renken, A. *J. Catal.* **2004**, *222*, 389.
(25) Grubert, G.; Hudson, M. J.; Joyner, R. W.; Stockenhuber, M. *J. Catal.* **2000**, *196*, 126.
(26) Heyden, A.; Bell, A. T.; Keil, F. J. *J. Catal.* **2005**, *233*, 26.
(27) Heyden, A.; Keil, F. J.; Peters, B.; Bell, A. T. *J. Phys. Chem. B* **2005**, *109*, 1857.
(28) Pérez-Ramírez, J.; Kapteijn, F.; Brückner, A. *J. Catal.* **2003**, *218*, 234.
(29) Gleaves, J. T.; Yablonsky, G. S.; Phanawadee, P.; Schuurman, Y. *Appl. Catal., A* **1997**, *160*, 55.
(30) Keipert, O. P.; Baerns, M. *Chem. Eng. Sci.* **1998**, *53*, 3623.
(31) Rothaemel, M. Ph.D. Thesis, Ruhr-Universität BochumBochum, 1995; p 140.
(32) Soick, M.; Wolf, D.; Baerns, M. *Chem. Eng. Sci.* **2000**, *55*, 2875.
(33) Sinkovek, R. F.; Madsen, N. K. *ACM Trans. Math. Software* **1975**, *1*, 232.
(34) Wolf, D.; Moros, R. *Chem. Eng. Sci.* **1997**, *52*, 1189.
(35) Press: W. H.; Flannery, B. P.; Teukolsky, S. A.; Vetterling, W. T. *Numerical Recipes in FORTRAN*; Cambridge University Press: Cambridge, U.K., 1992; p 402.
(36) Pérez-Ramírez, J.; Kondratenko, E. V.; Debbagh, M. N. *J. Catal.* **2005**, *233*, 442.
(37) Pirngruber, G. D.; Roy, P. K. *Catal. Today* **2005**, *110*, 199.
(38) Yakovlev, A. L.; Zhidomirov, G. M.; van Santen, R. A. *Catal. Lett.* **2001**, *75*, 45.
(39) Ryder, J. A.; Chakraborty, A. K.; Bell, A. T. *J. Catal.* **2003**, *220*, 84.
(40) Kondratenko, E. V.; Perez-Ramirez, J. *Appl. Catal., B* **2006**, *64*, 35.
(41) Kameoka, S.; Nobukawa, T.; Tanaka, S.; Ito, S.; Tomishige, K.; Kunimori, K. *Phys. Chem. Chem. Phys.* **2003**, *5*, 3328.
(42) Nobukawa, T.; Yoshida, M.; Kameoka, S.; Ito, S.; Tomishige, K.; Kunimori, K. *Catal. Today* **2004**, *93*−*95*, 791.
(43) Nobukawa, T.; Yoshida, M.; Kameoka, S.; Ito, S.; Tomishige, K.; Kunimori, K. *J. Phys. Chem. B* **2004**, *108*, 4071.
(44) Box, G. E. P.; Draper, N. R. *Empirical model-building and response surfaces*; Wiley & Sons: New York, 1987.
(45) Bates, D. M.; Watts, D. G. *Nonlinear regression analysis and its application*; John Wiley & Sons: New York, 1988.
(46) Pérez-Ramírez, J.; Santhosh, K. M.; Bruckner, A. *J. Catal.* **2004**, *223*, 13.
(47) Leglise, J.; Petunchi, J. O.; Hall, W. K. *J. Catal.* **1984**, *86*, 392.